Quantitative measurements of wave-equation illumination for evaluating acquisition geometries

Carlos Calderón-Macías*, Brent Mecham and Nick Bernitsas, *ION*

Summary

In complex geology settings, illumination studies can help in the acquisition design phase to QC and qualify competing survey designs. A wave equation approach for illumination handles complex models and the resulting data can undergo the processing flow applied to real data at the imaging stage. Typical factors to measure in illumination include dip and azimuth limits as a function of spatial location as well as overall amplitude distribution. In the proposed flow, we distribute regularly spaced hemi-spheres across the model to serve as reflectivity boundaries embedded in a background velocity model, which may incorporate salt bodies interpreted from legacy seismic data. The velocity model should overall represent with some degree of fidelity the real velocity in order for the illumination study to provide useful insights. The method we propose uses single scattering with acoustic finite differences to model synthetic seismograms, which we then migrate for illumination analysis. Amplitudes as a function of dip and azimuth are recovered from the migrated image to evaluate the illumination for a particular geometry layout. The analysis is helpful for selecting, among other things, a preferred acquisition azimuth orientation, aperture and maximum acquired offset. We show examples of the illumination procedure in a wide azimuth survey and a hypothetical complex velocity model. We present quantitative measurements from the illumination response that can be utilized for evaluating the geometries analyzed.

Introduction

Acquisition design benefits from illumination studies computed for target horizons beyond analyzing CMP fold coverage and offset and azimuth distribution across bins (e.g. Vermeer, 2012) in cases where a complex overburden is expected. The objective of illumination is to study amplitude variations along target horizons. Illumination studies are often ray-based (e.g. Lecomte et al., 2015), due to their efficiency and robustness. An alternative approach that can be more accurate in the case of complex geology is to use full wave-equation modeling for generating synthetic seismograms which can then be migrated for analyzing illumination (Cvetkovic et al., 2014). In our method, we use an approach that lets us decouple the velocity field as estimated from seismic data from hypothetical targets within the model, as it is commonly implemented with ray-based procedures. A source wavefield is propagated using acoustic finite differences through the background velocity model. The interaction of the incident wavefield with a reflectivity volume containing the target geology produces a scattered wavefield, which is forward propagated to the receivers with the same velocity field as used for the incident wavefield (or with a different velocity as it would be the case of waves converted from P to S). This form of modeling which is akin to Born modeling, produces seismograms without multiple scattering signal such as internal multiples from the target reflectors of the reflectivity model (although multiple scattering might still be generated from strong velocity contrasts present in the velocity model). Seismograms are then migrated with reverse time migration (RTM). For acquisition design purposes, we use relatively low frequencies to model and image the synthetic data (<35 Hz).

A number of procedures for evaluating illumination resulting from the interaction of the acquisition geometry, the geologic model and a source wavelet have been proposed in the literature. For instance, the use of ray-based point spread functions for measuring dip and resolution was proposed by Lecomte (2008). The focal beam method (Volker et al., 2001), which is also a target oriented method based on the common focus point technology, has been used for analyzing resolution and amplitude fidelity (e.g. Ishiyama and Blacquière, 2015). Alternatively, we propose a scheme in which hemi-spheres are regularly spaced within the reflectivity model at certain target depths. We then analyze the migrated image at the targets to derive attributes that help evaluate which acquisition geometry provides the best illumination. We have used this scheme to evaluate different geometry layout types and preferred shooting orientations such as narrow and wide azimuth surveys (NAZ and WAZ, respectively). We have found the approach to provide a relatively simple way for qualifying the illumination of a particular design. We next illustrate the steps of the approach with a hypothetical problem of an area with salt bodies with the objective of selecting a marine surface acquisition design that is optimal in terms of illuminating desired target zones, especially below salt.

Methodology and test example

Synthetic data are first computed given a background velocity model and anisotropy parameters when available, and a reflectivity model containing gridded horizons and a set of gridded hemi-spheres. The radius of the hemi-spheres should be smaller than the maximum offset in the survey (600 m in our experiments) and consistent with the modeled wavelengths in the data so that they can be imaged with a reasonable resolution. The hemi-spheres are placed at target depth levels such as base of sediments, bottom of salt and below salt. Laterally, hemi-spheres have enough separation between them to avoid signal overlap between neighbor

elements in the final image. As much as possible, overlapping between target horizons and hemi-spheres is minimized when constructing the reflectivity model. Figures 1a and 1b show a section from a velocity from a 3D model with shallow salt and a sample of the gridded reflectivity for computation of the synthetics seismograms. The reflectivity contains two target horizons at depths of about 6 and 9 km and four depth levels of hemi-spheres (from 5600 m to 11600 m at 2 km interval). Figure 2 shows a sample of a synthetic common shot gather (CSG) based on these two volumes for a WAZ geometry computed with 35 Hz of maximum frequency. Most of the signal observed in the data corresponds to single scattering energy from the hemi-spheres.

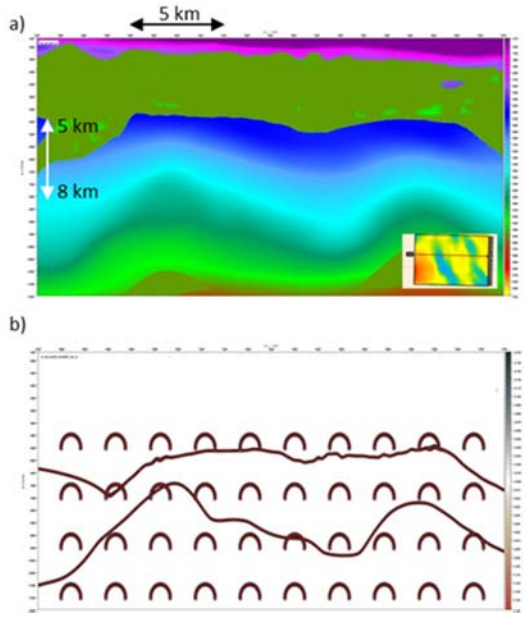

Figure 1. a) An inline section of the background velocity used for modeling. b) Reflectivity field with two target horizons and four hemi-sphere levels. The radius of the hemi-spheres is 600 m.

The second step of the flow consists of imaging the synthetic data with RTM. Figures 3a and 3b show an inline image of migrated data shot with EW (inline) and NS (xline) orientations, respectively. The maximum offset used for this test is 8 km. From comparing the two images, at the base of salt (first hemi-sphere level) we see that the two images are very similar, indicating no shooting orientation preference for the shallower target depths, where the illumination is mostly controlled by the salt body. There is an overall improved preservation of dips though for the data shot in the inline direction for larger depths. Figures 4a and 4b show a xline for the same two geometries (inline and xline shooting). For this case the geometry shot in the xline direction shows an advantage over the inline direction when comparing the maximum dips for the 2nd and 3rd depth levels.

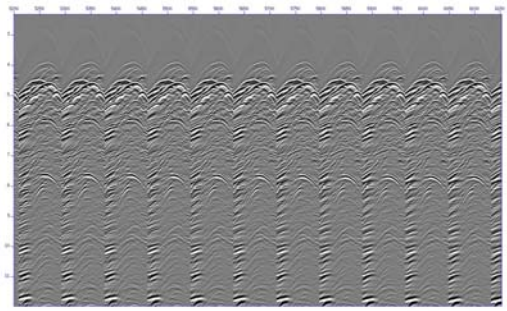

Figure 2. Sample shot of a WAZ geometry computed from the model in Figure 1. The maximum frequency of the data is 35 Hz.

To gain better insight into the effect of these two geometries for preserving dip after migration, the 3D dip field is computed and displayed in an aerial view for a selected region and depth level containing hemi-spheres (Figure 5). If dip is well preserved after migration (Figures 5b and 5c for inline and xline shooting orientations, respectively), it should match closely the dip computed from the target reflectivity model (Figure 5a), with values that range from 0° at the center of a hemi-sphere to relatively large angles at the edges (60° or higher). The dip slice from Figure 5 spans the depth range of 7000 m to 7600 m, the top and base of the 2nd level of hemi-spheres. In regions where a laterally continuous target horizon overlaps the depth window of the hemi-spheres as seen in Figures 2-4, the dip of the horizon is also displayed as seen in the top left corner of the panels in the left side of Figure 5. The base of the hemi-sphere is used to label the depth of study (7600 m in this case). The averaged dip resulting from stacking all the individual hemi-sphere elements appearing in the left panels is plotted on the right side of Figure 5 as a way to summarize overall the dip response for some selected regions. Qualitatively, the displays show that both geometries result in an illumination that has a NE-SW orientation, and that the xline geometry has a slight advantage over the inline shooting direction for preserving a high dip angle for a slightly wider azimuth range. To emphasize differences between the geometries, in these displays we have used a threshold of 5° of maximum difference between the target and the estimated dip and discarded grid points above the threshold by placing a zero value at those locations.

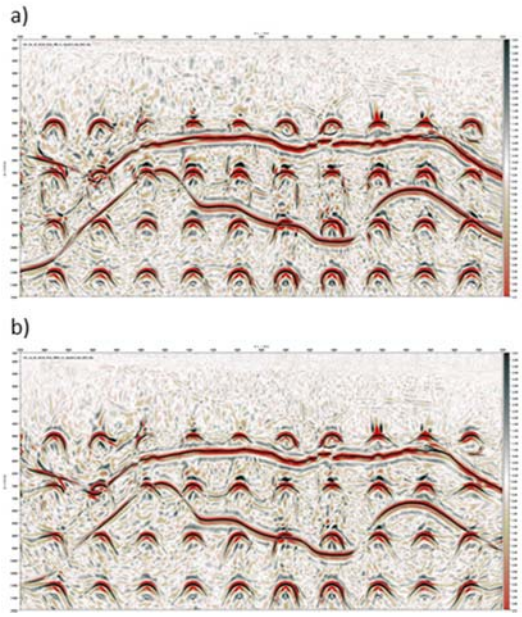

Figure 3. RTM EW (inline) images for WAZ surveys shot in the inline (a) and xline (b) directions. The maximum offset is 8 km.

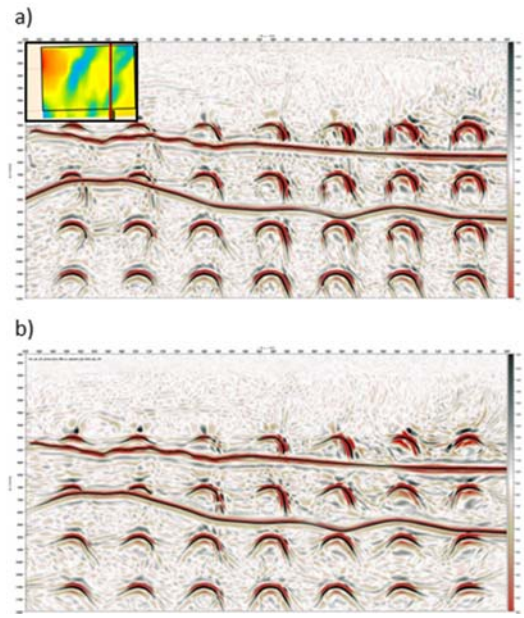

Figure 4. RTM NS (xline) images for WAZ surveys shot in the inline (a) and xline (b) directions. The maximum offset is 8 km.

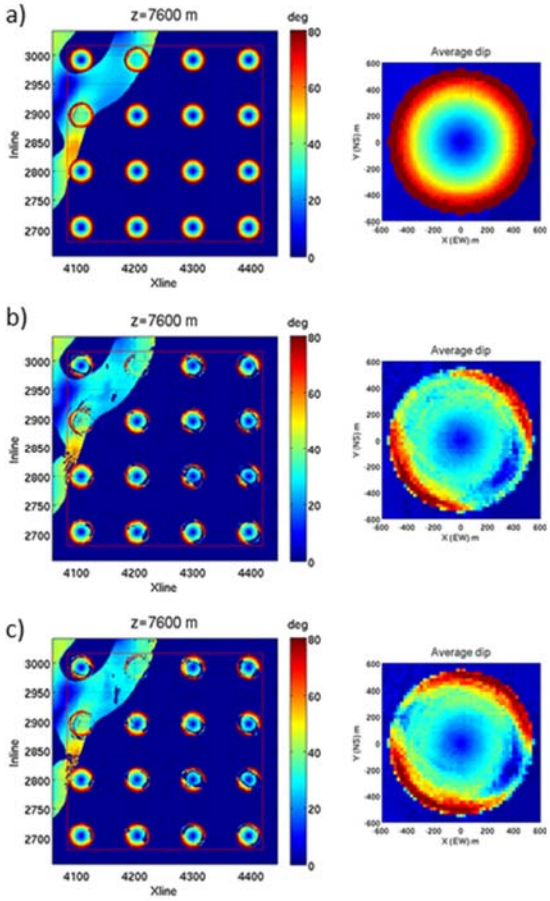

Figure 5. Sliced dip field for a region at the center of the model for the 2nd row of hemi-spheresand average dip response obtained from stacking all the ring responses for a) target reflectivity; b) RTM image for EW WAZ geometry and; c) RTM image for NS WAZ geometry. The colored region at the top left of the panels corresponds to the estimated dip of the 2nd horizon shown for the previous figures.

To provide quantitative estimates of dip for the target depth levels, maximum dip angle as a function of azimuth is retrieved from the average dip responses. Figures 6a and 6b show in polar form, the maximum dip angle as a function of azimuth from the average dip responses of Figures 5b and 5c, respectively. We compute an ellipticity factor as an estimate of how well dip is preserved across azimuth according to

$$E = (1- (max(\text{dip}) - avrg(\text{dip}))/max(\text{dip}))$$

where *max*(dip) corresponds to the maximum dip retrieved for any azimuth and *avrg*(dip) is the maximum dip averaged for all azimuths. A value of 1 indicates that the maximum dip retrieved is the same for all azimuths, whereas a small value indicates poor azimuth preservation across azimuth. The three quantities we then compare for competing acquisition geometries are the maximum and "minimum maximum" dip, and the ellipticity. In Figure 6, the maximum and minimum dip angles are similar but the NS shooting orientation has a value of ellipticity of 0.8 versus 0.73 for the EW direction. Figure 7 compares the dip response for the same depth level for WAZ and NAZ geometries over the same region, shot in the NS direction and with a longer maximum offset of 16 km. The NAZ and WAZ geometries retrieve a similar maximum dip angle with ellipticities of 0.82 and 0.92, respectively. For this model and at this depth level, increasing the offset from 8 to 16 km has an important impact for illumination in terms of dip preservation with azimuth.

Similar to the analysis of dip, amplitudes can be analyzed as a function of dip angle and azimuth. Amplitudes are retrieved following a similar procedure for slicing the dip field (not shown for brevity). For good illumination, amplitudes are to be relatively constant with azimuth and angle since the modeled synthetics do not carry AVO information. Since the dip is obtained from the analysis of dip of the migrated image, an inaccurate dip will potentially result in poor amplitude preservation.

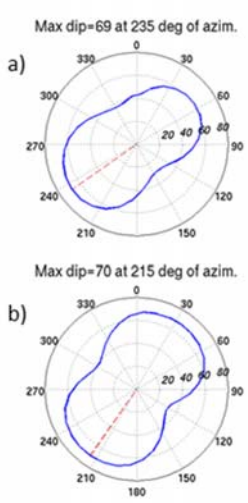

Figure 6. Polar display of maximum dip angle with azimuth for the EW (a) and NS (b) WAZ geometries at the target depth level of z=7600 m. The red dashed line shows the azimuth of maximum dip angle. The estimated ellipticity for these geometries are 0.73 (a) and 0.8 (b).

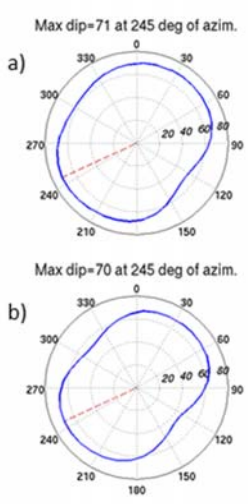

Figure 7. Polar display of maximum dip angle with azimuth for the NS WAZ (a) and NS NAZ (b) geometries at the target depth level of z=7600 m. The maximum offset is 16 km. The estimated ellipticity for these geometries are 0.92 (a) and 0.82 (b).

Conclusions

The proposed approach for evaluating illumination at the stage of acquisition planning uses the acoustic wave-equation to propagate the source and receiver wavefields given a gridded reflectivity and velocity model. The velocity model should follow some a priori information of the geology of the area of interest. We use hemi-spheres placed regularly in the model to evaluate dip preservation. Dip preservation has an important impact in general for imaging complex geology, resolving faults and mapping sediment-salt boundaries and sub-salt reflectors, as well as for velocity model building. To select an adequate geometry we use attributes such as maximum dip angle and ellipticity at various depth levels, averaging the dip response over regions of interest.

Acknowledgments

We thank ION for permission to publish this work. We thank Gulzar Aziz, Guoquan Chen, Greg Nash, and Susan Collins for their contributions.

References

Cvetkovic, M., C. Calderón-Macías, P. Farmer, and G. Watts, 2014, Efficient numerical modelling and imaging practices for aiding marine acquisition design and interpretation, First Break, 32, 3, 99-105.

Ishiyama, T. and G. Blacquière, 2015, 3-D shallow-water seismic survey evaluation and design using the focal-beam method: a case study offshore Abu Dhabi, Geophysical Prospecting, doi: 10.1111/1365-2478.12335

Lecomte, I., P. Lubrano Lavadera, I. Anell, S. J. Buckley, D. W. Schmid, and M. Heeremans, 2015, Ray-based seismic modeling of geologic models: Understanding and analyzing seismic images efficiently, Interpretation, Vol 3., No. 4, SAC71-SAC89.

Lecomte, I., 2008, Resolution and illumination analyses in PSDM: A ray based approach, The Leading Edge, 27, 650-663.

Vermeer, G.J.O. , 2012, *3-D seismic survey design*, Society Exploration Geophysicists.

Volker, A. W. F., G. Blacquière, A. J. Berkhout, and L. OngKiehong, 2001, Comprehensive assessment of seismic acquisition geometry by focal beams — Part II: Practical aspects and examples: Geophysics, 66, 918–931, doi: 10.1190/1.1444982.